SCIENTIFIC REPORTS

OPEN

SUBJECT AREAS:
HETEROGENEOUS CATALYSIS
POLYMER SYNTHESIS
SUSTAINABILITY

Received
24 April 2014

Accepted
6 June 2014

Published
27 June 2014

Correspondence and requests for materials should be addressed to R.W. (ruihu@fjirsm.ac.cn)

Shape-Controllable Formation of Poly-imidazolium Salts for Stable Palladium *N*-Heterocyclic Carbene Polymers

Huaixia Zhao, Liuyi Li, Yangxin Wang & Ruihu Wang

State Key Laboratory of Structural Chemistry, Fujian Institute of Research on the Structure of Matter, Chinese Academy of Sciences, Fuzhou, Fujian, 350002, China.

The imidazolium-based main-chain organic polymers are one of promising platforms in heterogeneous catalysis, the size and outer morphology of polymer particles are known to have important effects on their physical properties and catalytic applications, but main-chain ionic polymers usually generate amorphous or spherical particles. Herein, we presented a versatile and facile synthetic route for size- and shape-controllable synthesis of main-chain poly-imidazolium particles. The wire-shaped, spherical and ribbon-shaped morphologies of poly-imidazolium particles were readily synthesized through quaternization of bis-(imidazol-1-yl)methane and 2,4,6-tris(4-(bromomethyl)phenyl)-1,3,5-triazine, and the modification of their size and morphology were realized through adjusting solvent polarity, solubility, concentration and temperatures. The direct complexation of the particles with $Pd(OAc)_2$ produced ionic polymers containing palladium N-heterocyclic carbene units (NHCs) with intactness of original morphologies. The particle morphologies have a significant effect on catalytic performances. Wire-shaped palladium-NHC polymer shows excellent catalytic activity and recyclabilty in heterogeneous Suzuki-Miyaura cross-coupling reaction.

As useful ligands in organometallic chemistry and catalysis, *N*-heterocyclic carbene (NHC) complexes have attracted considerable attention due to their unique sigma donor properties and remarkable similarity to electron-rich phosphine ligands[1–3]. To improve recyclability of such NHC complexes, great efforts have been devoted to develop heterogeneous NHC organometallic catalytic systems[3–7]. Imidazolium-based ionic salts are well known to be excellent precursors of metal NHCs, and various solid supports containing imidazolium groups have been used as precursors of heterogeneous palladium NHCs[3–6]. In the context, di- or poly-cationic imidazolium salts were well known to possess superior performances over monocationic analogues, but heterogeneous catalytic systems consisting of stable chelating palladium NHC units were seldom explored[3,4], despite the discrete chelating palladium NHC complexes were frequently investigated in catalysis[2]. Very recently, a series of metal-organic frameworks (MOFs) containing methylene-bridged bis-imidazolium groups were reported[8], but the relative instability of these MOFs against moisture, acid or base have restricted the scope of catalytic applications.

It is known that organic polymers usually display high stability even under rigorous conditions owing to the existence of strong covalent bonds[9,10]. The imidazolium-based main-chain organic networks may be constructed through *in situ* formation of imidazolium rings[11] or polymerization of organic building blocks containing imidazolium units[12,13]. In contrast, the quaternization of bis- or multi-imidazole ligands is the most simple route for the synthesis of poly-imidazolium salts (PIS). Recently, a series of poly-imidazolium spherical particles were prepared through the quaternization of semirigid bis- or tri-imidazole ligands[14,15]. The main-chain ionic polymers may serve as excellent precursors for the synthesis of polymeric NHC particles and palladium NHC polymers, but the spherical particles are not strong enough for palladium-catalyzed heterogeneous catalysis. The outer shape of particles is reported to have an important effect on their physical properties and ultimate applications, but main-chain organic polymers are readily to spontaneously form spherical or amorphous particles[14–17]. In comparison with well-developed inorganic[18] and coordination polymer particles[19], the controllable synthesis of morphologies in poly-imidazolium particles is still untapped. In our continuous efforts to develop heterogeneous catalytic

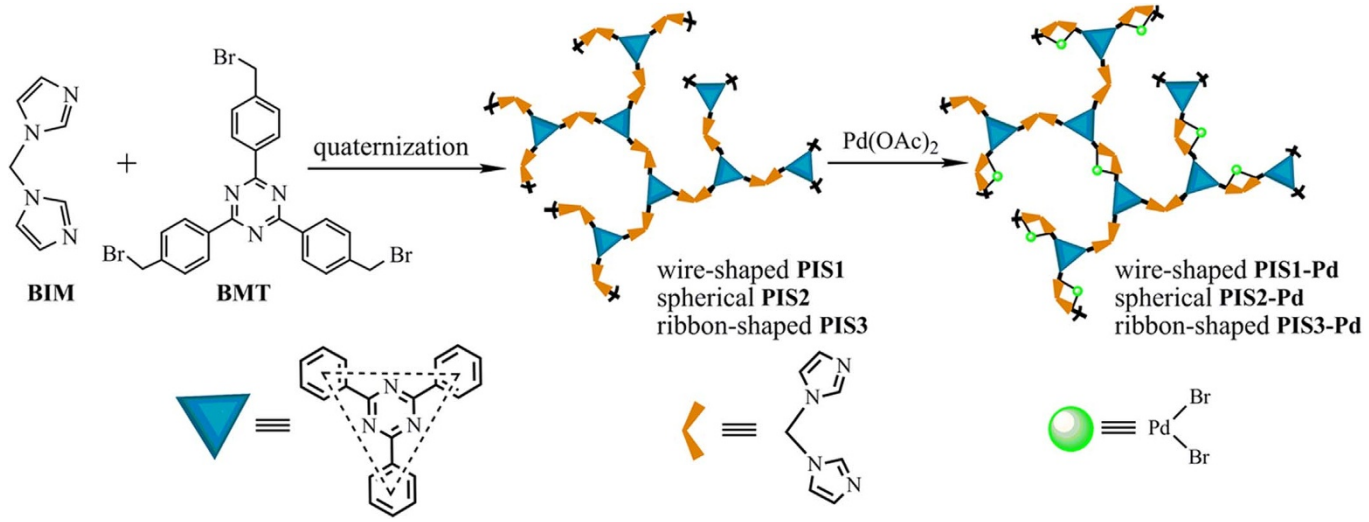

Figure 1 | **General synthetic route of PIS and PIS-Pd.**

systems[20], herein, we present a new strategy for controllable synthesis of wire-shaped (PIS1), spherical (PIS2) and ribbon-shaped (PIS3) poly-imidazolium particles from quaternization of 2,4,6-tris(4-(bromomethyl)phenyl)-1,3,5-triazine and bis-(imidazol-1-yl)methane (Figure 1). The main-chain imidazolium-based particles may serve as effective precursors for the formation of polymers containing stable palladium NHC units, and no obvious changes of morphology and loss of catalytic activity were observed after wire-shaped particles were used over 13 times in palladium-catalyzed Suzuki-Miyaura cross-coupling reaction.

Results

Design approach. It is well known that 1,3,5-triazine core is a promising linker in the construction of metal-organic frameworks[21] and porous organic frameworks[22]. The core usually possesses strong electron affinity, the covalent linkage with aromatic groups is inclined to induce an effective conjugation, resulting in the formation of π...π packing interaction and decrement of solubility of resultant compounds. The semirigid tripodal 2,4,6-tris(4-(bromomethyl)phenyl)-1,3,5-triazine (BMT) is readily obtained through cyclotrimerization of *p*-bromomethylbenzonitrile[23]. Flexible bis-(imidazol-1-yl)methane (BIM) is easily available through alkylation of imidazole[24], and the subsequent quaternization may produce dicationic bis-(imidazolium)methane, which is a popular precursor for the formation of stable palladium NHC containing six-membered ring[2–4]. The combination of BMT and BIM may form main-chain organic frameworks containing bicationic bis-(imidazolium)methane units.

Syntheses. As shown in Figure 2a, a mixture of 0.1 mmol BMT and 1.5 equivalent of BIM in 5 mL MeCN at 85°C gave rise to wire-shaped PIS1. When MeCN volume was increased to 20 mL, concomitant formation of spherical particles was observed (Figure 3a). Further increment of MeCN volume to 40 mL and 60 mL resulted in the formation of more spherical particles (Figures 3b and 3c), which is probably ascribed to incomplete solubility of BMT in MeCN at 85°C. Interestingly, when reaction temperature was elevated to 100°C, total spherical particles of 500–800 nm (PIS2) were generated in 40 mL MeCN (Figure 2d), in which BMT is well dissolved. BMT is also soluble in THF, dioxane and DMF, but the polarity of these solvents is different, which encourages us to explore the formation of poly-imidazolium particles in these solvents. As expected, when 10 mL DMF was used as a solvent instead of MeCN at 85°C, spherical particles of 0.5–1 μm were formed (Figure 3d). The decrement of DMF volume to 5 mL generated larger spherical particles of 2–3 um (Figure 3e). However, when 5mL THF was used as a solvent at 85°C, ribbon-shaped particles (PIS3) were formed (Figure 2g). The elevation of temperature or the increment of THF volume has not resulted in concomitant formation of other morphological particles. Similar results were also achieved in dioxane (Figure 3f).

Structural characterization. All of PIS are insoluble in water and common organic solvents. Their particle size and morphology are illustrated by SEM analyses (Figures 2 and 3), and their formation is clearly confirmed by solid-state ^{13}C NMR spectra, IR and elementary analysis. Solid-state ^{13}C NMR and IR spectra of PIS1, PIS2 and PIS3 are nearly identical with each other. The characteristic peaks of quaternary imidazolium appear around 1159 and 763 cm^{-1} in their IR spectra (Figure S1)[14].

In solid-state ^{13}C NMR spectra of PIS, the peak of 2-positioned carbon of imidazolium is around 138 ppm, and the peak at 169 ppm is assigned to triazine carbon atoms, methylene of BMT and BIM affords the characteristic peaks at 53 and 62 ppm, respectively (Figure S2). N_2 adsorption experiments show that the surface area of PIS1, PIS2 and PIS3 are 9.56, 5.97 and 8.43 $m^2 \cdot g^{-1}$, respectively. Elementary analyses reveal that the measurement values of carbon (44.58–46.91%) and nitrogen (13.32–14.23%) are slightly lower than the expected values (C, 51.0; N, 15.5%) owing to the presence of guest molecules, which is further confirmed by TGA. Obvious weight losses of 4.4, 4.4 and 7.1% were observed before 110°C in TGA curves of PIS1, PIS2 and PIS3, respectively. The poly-imidazoliun particles are stable before 300°C (Figure S3).

Palladium carbene polymers. Similar to the reported palladium(II) NHCs from discrete methylene-bridged bis(imidazolium) salts[2–4], PIS were readily transformed into organometallic polymers through a concerted process of deprotonation and subsequent metalation. As shown in Figure 1, the direct treatment of PIS with $Pd(OAc)_2$ in DMSO produced the corresponding palladium NHC polymers (PIS-Pd) as yellow solids. ICP analyses show that palladium contents in PIS1-Pd, PIS2-Pd and PIS3-Pd are 0.76, 0.64 and 0.73 mmol/g, respectively, corresponding to 54, 45 and 51% of total imidazolium group binding to palladium(II), respectively. It should be mentioned that 80% of theoretical $Pd(OAc)_2$ was used in the preparation of PIS-Pd. The reaction of PIS and $Pd(OAc)_2$ was also attempted using a 1 : 2 molar ratio of palladium(II) to imidazolium based on the desirable formation of chelating palladium-NHC units, but palladium black was observed after the reaction. As a result, the use of low palladium loading not only may

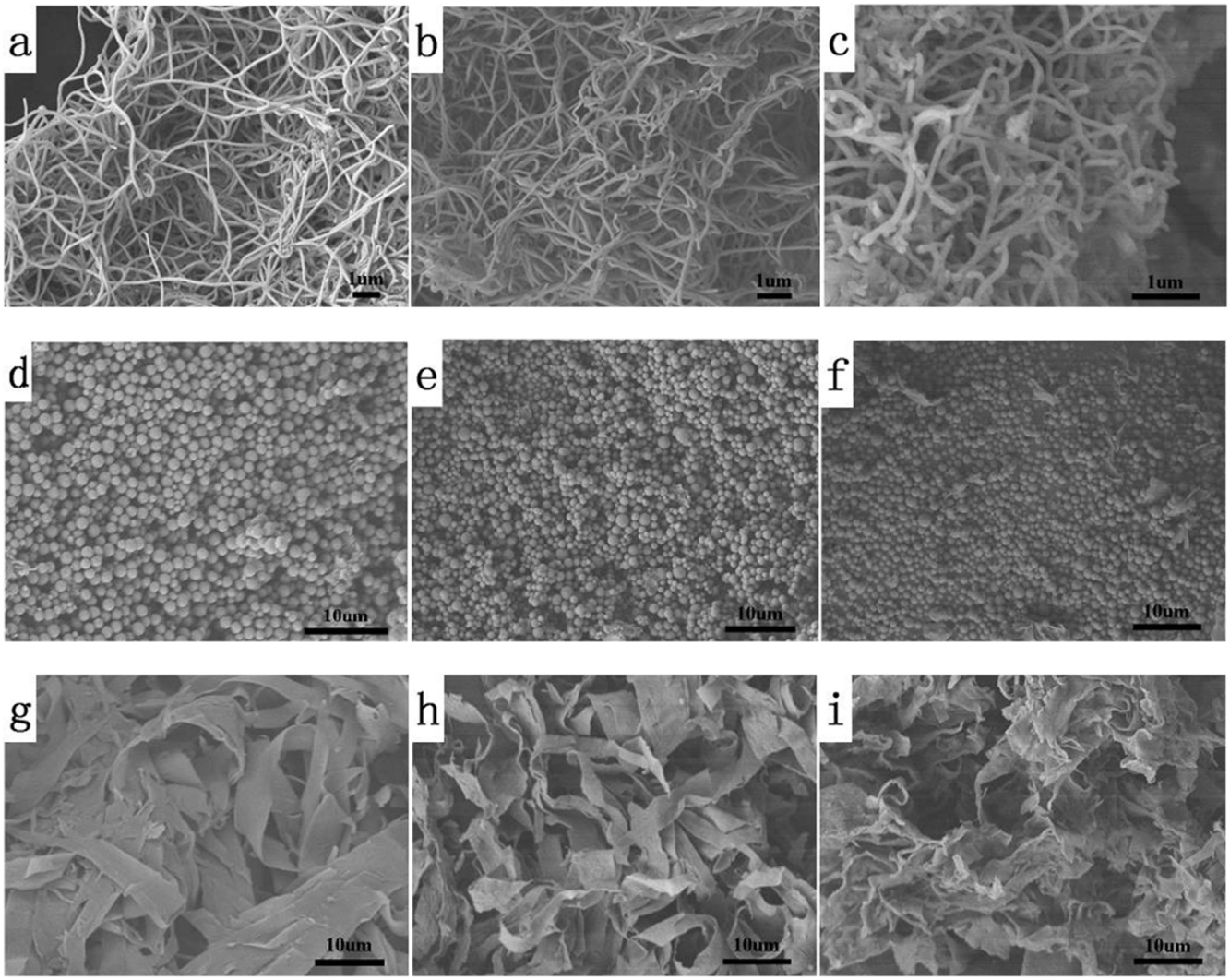

Figure 2 | SEM images for (a) wire-shaped PIS1; (b) wire-shaped PIS1-Pd; (c) wire-shaped PIS1-Pd after catalytic cycle for 13 runs; (d) spherical PIS2; (e) spherical PIS2-Pd; (f) spherical PIS2-Pd after catalytic reaction; (g) ribbon-shaped PIS3; (h) ribbon-shaped PIS3-Pd; (i) ribbon-shaped PIS3-Pd after catalytic reaction.

avoid the formation of palladium black and improve the utilization efficiency of palladium in the catalytic reaction, but also may enhance the dispersion of PIS-Pd in H_2O/DMF with help of imidazolium and bromide.

In comparison with PIS, the peak of 2-positioned carbon of imidazolium at 138 ppm is weakened in solid-state ^{13}C NMR of PIS-Pd, while a new signal around 160 ppm was observed (Figure S4), which is attributed to the formation of palladium NHC in 2-positioned carbon of imidazolium ring[17]. The peaks of quaternary imidazolium at 763 and 1159 cm^{-1} are also weakened in IR spectra of PIS-Pd, while a new band at 1233 cm^{-1} appears (Figure S1). Other peaks of PIS-Pd in IR and solid-state ^{13}C NMR are almost identical with those in PIS, indicating the preservation of structural frameworks after the formation of palladium NHC units. SEM analyses further confirm that there are no morphological changes between PIS-Pd and PIS (Figure 2). The thermal stability of PIS-Pd is similar to that of PIS (Figure S5).

XPS spectra corroborate the only existence of palladium(II) in PIS-Pd, with the peaks of binging energy at 337.9 ($3d_{5/2}$) and 343.0 eV ($3d_{3/2}$) (Figure S6)[15]. In comparison with Pd $3d_{5/2}$ peak of free $Pd(OAc)_2$ at 338.4 eV, the peak of palladium(II) in PIS-Pd is negatively shifted about 0.5 ev, which further confirms the formation of palladium NHC units in PIS-Pd. STEM-mapping show that nitrogen, bromine and palladium are uniformly distributed on PIS-Pd despite the difference of their morphologies (Figure S7).

Catalysis. In order to investigate the effects of wire-shaped, spherical and ribbon-shaped morphologies on catalytic performances, Suzuki-Miyaura cross-coupling reaction between 4-bromoacetophenone and phenylboronic acid was evaluated in the presence of K_2CO_3 in DMF/H_2O. As shown in Table 1, a quantitative GC yield was achieved for wire-shaped PIS1-Pd (entry 1), while spherical PIS2-Pd and ribbon-shaped PIS3-Pd gave 4-acetylbiphenyl in 82 and 90% GC yields, respectively (entries 2 and 3). This effect was further explored through the reaction time-screening conversion curves. As shown in Figure S8, PIS1-Pd, PIS2-Pd and PIS3-Pd possess an induction period of reaction, but conversion of 4-bromoacetophenone in PIS1-Pd is higher than that in PIS2-Pd and PIS3-Pd. The reaction ratio of PIS3-Pd is lower than that in PIS2-Pd in 2 h owing to relatively long induction time, but conversion of 4-bromoacetophenone in PIS3-Pd becomes higher than that in PIS2-Pd after 2.5 h. The highest catalytic activity in PIS1-Pd is probably ascribed to larger conatct areas with the reactants of wire-shaped particles than spherical PIS2-Pd, while ribbon-shaped PIS3-Pd has a low dispersion in DMF/H_2O, which results in the longest induction period of the reaction. With the continuation of reaction, its reaction

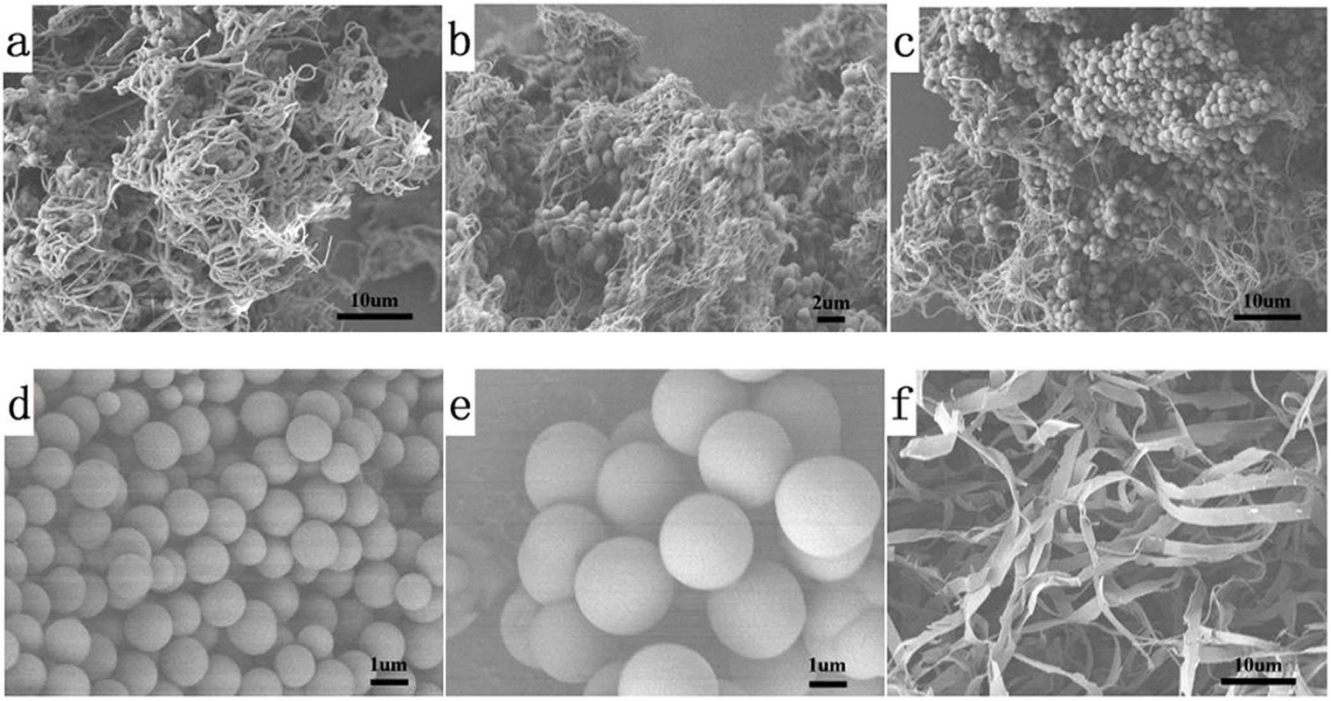

Figure 3 | SEM images for PIS formed at different conditions. (a) 20 mL MeCN at 85°C; (b) 40 mL MeCN at 85°C; (c) 60 mL MeCN at 85°C; (d) 10 mL DMF at 85°C; (e) 5 mL DMF at 85°C; (f) 5 mL dioxane at 85°C.

rate gradually enhances, and finally surpasses that in spherical PIS2-Pd. Interestingly, SEM analyses show the respective original morphologies of PIS1-Pd, PIS2-Pd and PIS3-Pd have no obvious variation after catalytic reaction (Figures 2c, 2f and 2i). Moreover, their palladium XPS analyses show no detectable Pd(0) species are formed (Figure S6), which is probably ascribed to reoxidiation of Pd(0) after catalytic reaction and strong chelating ability of bis-carbene units in PIS-Pd.

Table 1 | Suzuki-Miyaura cross-coupling reactions of aryl bromides and aryl boronic acid[a)]

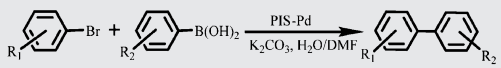

Entry	Catalyst	R_1	R_2	Yield [%][b)]
1	PIS1-Pd	*p*-$COCH_3$	H	100(98)
2	PIS2-Pd	*p*-$COCH_3$	H	82
3	PIS3-Pd	*p*-$COCH_3$	H	90
4	PIS1-Pd	*p*-NO_2	H	100
5	PIS1-Pd	*p*-CN	H	100(98)
6	PIS1-Pd	*p*-F	H	100
7	PIS1-Pd	*p*-NH_2	H	100(99)
8	PIS1-Pd	*p*-OH	H	100(78)
9	PIS1-Pd	*p*-OCH_3	H	100(99)
10	PIS1-Pd	*m*-OCH_3	H	98
11	PIS1-Pd	*o*-OCH_3	H	75
12	PIS1-Pd	*p*-$COCH_3$	*p*-F	100(98)
13	PIS1-Pd	*p*-$COCH_3$	*m*-F	100(99)
14	PIS1-Pd	*p*-$COCH_3$	*p*-OCH_3	100(99)
15	PIS1-Pd	*p*-$COCH_3$	*m*-OCH_3	100(90)
16	PIS1-Pd	*p*-$COCH_3$	*p*-CH_3	100(94)
17	PIS1-Pd	*p*-$COCH_3$	*m*-CH_3	100(98)
18[c)]	PIS1-Pd	1,4-dibromobenzene	H	100(87)
19[c)]	PIS1-Pd	2,6-dibromopyridine	H	100(95)
20[d)]	PIS1-Pd	*p*-$COCH_3$	H	100
21[e)]	PIS1-Pd	*p*-$COCH_3$	H	98

[a)]Reaction conditions: Aryl bromides (0.2 mmol), aryl boronic acid (0.3 mmol), K_2CO_3 (0.4 mmol) and PIS-Pd (1 mol%) in water (1.0 mL) and DMF(0.5 mL) at 100°C for 3 h; b) GC yields, isolated yields are given in parentheses; [c)] 120°C for 12 h; [d)] one drop of Hg was added; [e)] PVP with PVP/[Pd] molar ratio of 400 was added.

The scope and generality of substrates were further explored using PIS1-Pd as a precatalyst. The effect of varying aryl bromides was initially examined by using phenylboronic as a substrate. The reactions of the electron-deficient and electron-rich aryl bromides with phenylboronic acid provided the desirable products in quantitative yields (entries 4–9), while the sterically hindered 3-bromoanisole and 2-bromoanisole gave the resultant products in 98 and 75% GC yields, respectively (entries 10 and 11). The coupling reactions of 4-bromoacetophenone with other *meta*- and *para*-substituted aryl boronic acids were also performed, and the corresponding biaryl products were obtained in quantitative GC yield, regardless of the electronic and steric nature of aryl boronic acids (entries 12–17). Interestingly, the disubstituted aryl bromides, such as 1,4-dibromobenzene and 2,6-dibromopyridine, are also reactive in the catalytic system, *p*-terphenyl and 2,6-diphenylpyridine were obtained in 87 and 95% isolated yields in 120°C for 12 h, respectively (entries 18 and 19).

The stability and reusability are very important factors for a heterogeneous catalytic system. The good catalytic activity of PIS1-Pd encourages us to investigate its recyclability. After coupling reaction between 4-bromoacetophenone and phenylboronic acid was finished, the product was isolated through simple extraction while the remaining catalytically active species were separated by centrifugation, dried in vacuo and then employed for the next run with charge of fresh substrates. The catalytic system was used at least 13 times, and no detectable loss of catalytic activity was observed (Figure 4). Moreover, wire-shaped morphology of PIS1-Pd is intact (Figure 1i). ICP analyses show 0.005wt% and 0.001wt% of total Pd content are leached into solution in the first run and second run, respectively. Hot filtration experiment was also examined. When reaction was performed for 1 h, 4-acetylbiphenyl was obtained in 87% GC yield. After the reaction mixture was quickly filtrated at 100°C, the filtrate continued to react under the same conditions for additional 2 h, and GC yield of 4-acetylbiphenyl was maintained at 88%. The absence of catalytic activity in hot filtrate solution further

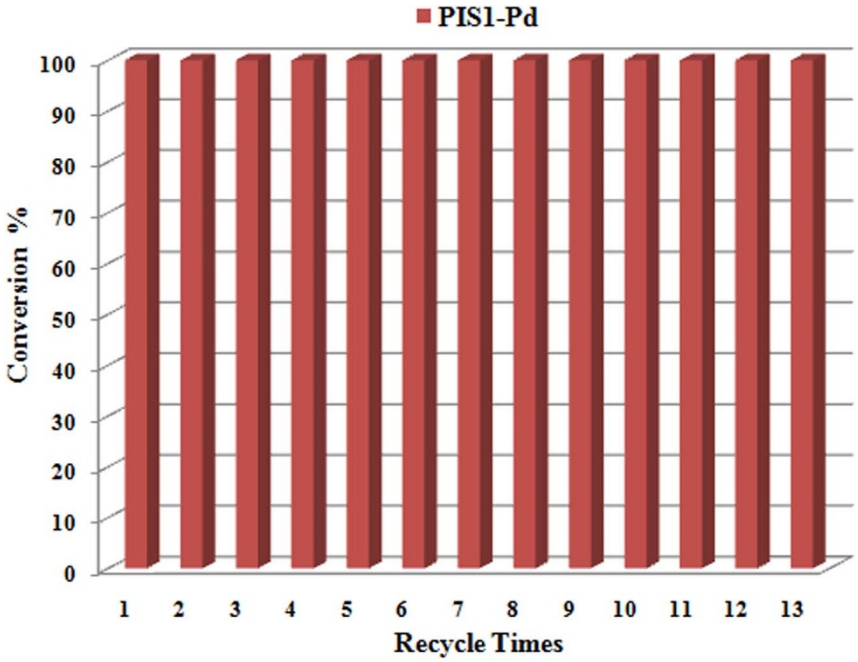

Figure 4 | Recyclability of wire-shaped PIS1-Pd in Suzuki-Miyaura cross-coupling reaction. Reaction conditions: 4-bromoacetophenone (0.2 mmol), phenylboronic acid (0.3 mmol), base (0.4 mmol), PIS1-Pd (1 mol%) in H_2O (1.0 mL) and DMF (0.5 mL) at 100°C for 3 h.

suggests negligible leaching of the catalytically active species into solution phase from PIS1-Pd during the reaction and separation. To further ensure that PIS1-Pd represents the catalytic active species rather than free palladium that is dissociated from the polymers during reaction, mercury drop and poisoning test were performed. When one drop of mercury or polyvinylpyridine (PVP) (PVP/Pd = 400 : 1) was added under the same conditions, no obvious effect on catalytic reaction was observed (Table 1, entries 20 and 21). These results show Suzuki-Miyaura reaction catalyzed by PIS1-Pd is a heterogeneous process.

Discussion

The formation mechanism of main-chain poly-imidazolium particles with different morphologies was proposed according to growth mechanism of inorganic particles with controllable morphologies[18,25], the formation of wire-shaped PIS1 and ribbon-shaped PIS3 is probably ascribed to kinetic dissimilarity of different directions in the process of the connection of BIM and IMB, which results in anisotropic evolution of the particles. Their growth process can be speculated to take place step by step according to different steric and electronic situations[20]. As shown in Figure 5, the growth of poly-imidazolium particles in the directions of length, width and thickness can be postulated as the formation of 1D chain by 1 : 1 connection of BMT and BIM, interconnection of 1D chains to 2D network, and further connection to 3D network, respectively[26,27]. The processes will occur at the same time and compete with each other. Because BMT is partially dissolved in 5 mL MeCN at 85°C, the anisotropic evolution can be induced efficiently by gradual dissolution of BMT in the process of the connection of BMT and BIM. The evolution rate in the direction of length (v_a) is drastically faster owing to the limit of BMT concentration[25], while high polarity of MeCN may induce identical evolution of the chiasmal multicharged networks in the directions of width (v_b) and thickness (v_c), generating wire-shaped poly-imidazolium particles. With increment of MeCN volume, the concentration of BIM is lowered and more BMT is dissolved, and when certain critical values are reached, concomitant formation of spherical particles appears owing to spontaneous isotropic evolution in part. When BMT is completely dissolved in 40 mL MeCN at 100°C, the preferential growth in the direction of length disappears completely, resulting in the formation of uniform spherical particles. In the case, the connection rate of BMT and BIM in the directions of length, width and thickness is identical with each other. The polarity of DMF is slightly higher than that of MeCN, and BMT has a good solubility in DMF. Thus, total spherical particles are obtained in DMF, moreover, particle size may be controlled through variation of BMT concentration. Alternatively, BMT is also soluble in THF and dioxane, but less polarity of THF and dioxane easily leads to fast precipitation of PIS from the mother solution. The growth of particles in the directions of width and thickness is inhibited at different levels, generating ribbon-shaped poly-imidazolium particles.

In conclusion, we presented a series of wire-shaped, spherical and ribbon-shaped poly-imidazolium particles, and their sizes and morphologies were readily modified through judicial selection of solvent, concentration and temperature. Palladium(II) was easily incorporated into parent poly-imidazolium salts by direct complexation with $Pd(OAc)_2$ with their original morphologies well maintained. An obvious effect of particle morphologies on catalytic performances was observed. Wire-shaped palladium-NHC particles show excellent catalytic activity and recyclability in heterogeneous catalysis with negligible palladium leaching and the intactness of original morphology. As a result, this study not only provides an optimized route for size- and shape-controllable synthesis of poly-imidazolium particles, but also widens the scope of palladium NHC complexes.

Method

Preparation of wire-shaped PIS1. To a suspension of BMT (0.10 mmol, 58.8 mg) in 4 mL MeCN at 85°C, a solution of BIM (0.15 mmol, 22.2 mg) in 1 mL MeCN was added. After the mixture was stirred at this temperature for 10 h, white insoluble precipitate was formed. The precipitate was collected by centrifugation, washed with MeCN (2 × 30 mL) and dried in vacuo. Yield: 73 mg (90%). IR (KBr, cm^{-1}): 3064(m), 1736(w), 1618(vw), 1587(vw),1520(s), 1413(m), 1366(m), 1181(m), 1159(m), 1109(vw), 1017(m), 945(w), 874(w), 796(m), 768(m), 761(m), 595(w), 509(w). Elemental analysis calculated (%) for $(C_{69}H_{60}N_{18}Br_6)_n$ (1620.76): C 51.13, H 3.73, N 15.56; found: C, 46.15, H, 4.25, N, 13.81.

Preparation of spherical PIS2. The synthetic procedure was similar to that of PIS1 except that total volume of MeCN was increased to 40 mL and temperature was elevated to 100°C. Yield: 65 mg (80%). IR (KBr, cm^{-1}): 3064(m), 1736(w), 1618(vw), 1587(vw), 1520(s), 1413(m), 1366(m), 1181(m), 1159(m), 1109(vw), 1017(m), 945(w), 874(w), 796(m), 768(m), 761(m), 595(w), 509(w). Elemental analysis

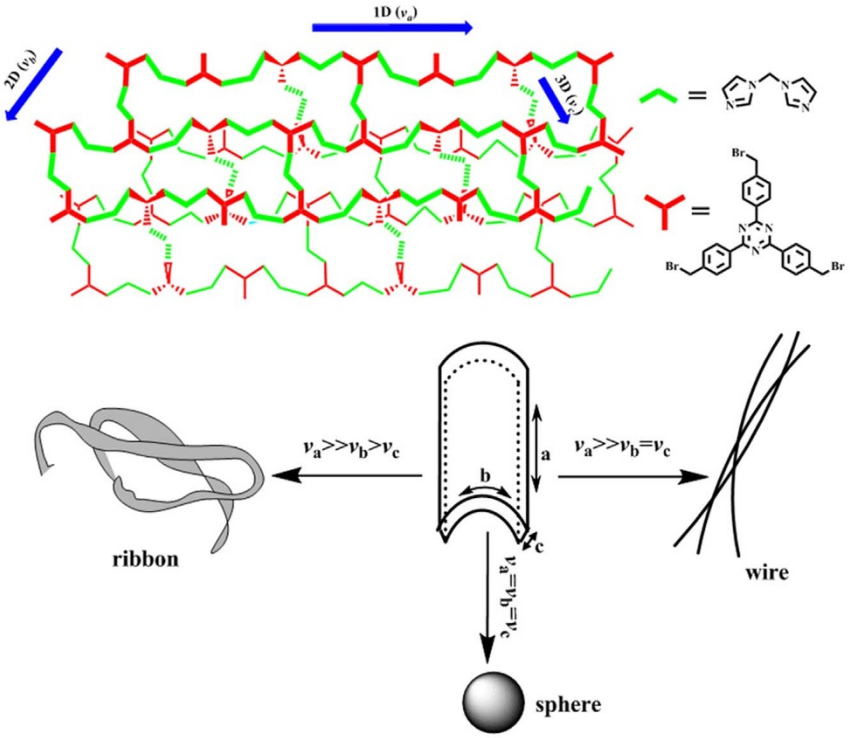

Figure 5 | The plausible mechanism for PIS formation.

calculated (%) for $(C_{69}H_{60}N_{18}Br_6)_n$ (1620.76): C 51.13, H 3.73, N 15.56; found: C,46.91, H, 4.66, N,14.23.

Preparation of ribbon-shaped PIS3. The synthetic procedure was similar to that of PIS1 except that MeCN was replaced by THF. Yield: 52 mg (64%). IR (KBr, cm^{-1}): 3064(m), 1736(w), 1618(vw), 1587(vw), 1520(s), 1413(m), 1366(m), 1181(m), 1159(m), 1109(vw), 1017(m), 945(w), 874(w), 796(m), 768(m), 761(m), 595(w), 509(w). Elemental analysis calculated (%) for $(C_{69}H_{60}N_{18}Br_6)_n$ (1620.76): C 51.13, H 3.73, N 15.56; found: C, 44.58, H, 4.13, N, 13.32.

Preparation of wire-shaped PIS1-Pd. To a stirring solution of $Pd(OAc)_2$ (45 mg) in DMSO (120 mL), PIS1 (150 mg) was added. The mixture was continuously stirred at 25°C for 3 h, 70°C for 12 h, and 100°C for 6 h. The yellow precipitate was isolated by filtration and further Soxhlet extraction with dichloromethane, and then dried in vacuo at 80°C for 12 h. Yield: 150 mg (77%). Pd content is 8.07 wt% (0.76 mmol/g) as determined by ICP. IR (KBr, cm^{-1}): 3094(m), 1736(w), 1618(w), 1587(w), 1520(s), 1413(m), 1366(m), 1233(m), 1181(m), 1159(m), 1109(w), 1017(m), 945(w), 874(w), 796(m), 760(m), 766(vw), 595(w), 509(w). Elemental analysis calculated (%) for $(C_{69}H_{54}Br_6N_{18}Pd_3)_n$ (1933.98): C 42.85, H 2.81, N 13.04; found: C, 41.20, H, 3.80, N, 12.04.

Preparation of spherical PIS2-Pd. The synthetic procedure was similar to that of PIS1-Pd except that PIS1 was replaced by PIS2. Yield: 67%. Pd content in PIS2-Pd is 6.76 wt% (0.64 mmol/g) as determined by ICP. IR (KBr, cm^{-1}): 3094(m), 1736(w), 1618(w), 1587(w), 1520(s), 1413(m), 1366(m), 1233(m), 1181(m), 1159(m), 1109(w), 1017(m), 945(w), 874(w), 796(m), 760(m), 766(vw), 595(w), 509(w). Elemental analysis calculated (%) for $(C_{69}H_{54}Br_6N_{18}Pd_3)_n$ (1933.98): C 42.85, H 2.81, N 13.04; found: C, 41.58, H, 3.88, N, 12.24.

Preparation of ribbon-shaped PIS3-Pd. The synthetic procedure was similar to that of PIS1-Pd except that PIS1 was replaced by PIS3. Yield: 92%. Pd content in PIS3-Pd is 7.80 wt% (0.73 mmol/g) as determined by ICP. IR (KBr, cm^{-1}): 3094(m), 1736(w), 1618(w), 1587(w), 1520(s), 1413(m), 1366(m), 1233(m), 1181(m), 1159(m), 1109(w), 1017(m), 945(w), 874(w), 796(m), 766(vw), 595(w), 509(w). Elemental analysis calculated (%) for $(C_{69}H_{54}Br_6N_{18}Pd_3)_n$ (1933.98): C 42.85, H 2.81, N 13.04; found: C, 40.57, H, 3.96, N, 12.20.

General procedures for Suzuki-Miyaura cross-coupling reaction. A 25 mL reactor equipped with a screw cap was charged with aryl bromide (0.2 mmol), aryl boronic acid (0.3 mmol), K_2CO_3 (0.4 mmol) and palladium catalyst (1 mol% Pd) in H_2O (1.0 mL) and DMF (0.5 mL). The reaction mixture was stirred at 100°C for 3 h. The resultant mixture was cooled with icy water, and the product was extracted with ethyl acetate (3 × 5 mL). The combined organic layer was dried over anhydrous Na_2SO_4, and then the solvent was removed under the reduced pressure. The crude product was purified by flash column chromatography on silica gel to afford the desired product. The identity of the product was confirmed by comparison with literature spectroscopic data.

Recyclability test of wire-shaped PIS1-Pd. A mixture of 4-bromoacetophenone (0.2 mmol), phenylboronic acid (0.3 mmol), PIS1-Pd (1 mol%) and K_2CO_3 (0.4 mmol) in H_2O (1.0 mL) and DMF(0.5 mL) was stirred at 100°C for 3 h. After cooling with icy water, the crude product was extracted with ethyl acetate (3 × 5 mL) and the conversion was determined by GC. The residual solid was separated by centrifugation, washed by ethyl acetate and dichloromethane, and then transferred to the reactor in diethyl ether and dried in vacuo. The recovered catalyst was used directly for the next run.

Hot filtration test of wire-shaped PIS1-Pd. A mixture of 4-bromoacetophenone (0.2 mmol), phenylboronic acid (0.3 mmol), PIS1-Pd (1 mol%) and K_2CO_3 (0.4 mmol) in H_2O (1.0 mL) and DMF (0.5 mL) was stirred at 100°C for 1 h. The resultant mixture was quickly filtered, and the filtrate continued to react at 100°C for another two hours. After cooling with icy water, the crude product was extracted with ethyl acetate (3 × 5 mL) and the conversion was determined by GC.

1. Valente, C. *et al.* The development of bulky palladium NHC complexes for the most-challenging cross-coupling reactions. *Angew. Chem. Int. Ed.* **51**, 3314–3332 (2012).
2. Lin, J. C. Y. *et al.* Coinage metal-*N*-Heterocyclic carbene complexes. *Chem. Rev.* **109**, 3561–3598 (2009).
3. Ranganath, K. V. S., Onitsuka, S., Kumar, A. K. & Inanaga, J. Recent progress of *N*-heterocyclic carbenes in heterogeneous catalysis. *Catal. Sci. Technol.* **3**, 2161–2181 (2013).
4. Schwarz, J. *et al.* Polymer-supported Carbene complexes of palladium: Well-defined, air-stable, recyclable catalysts for the heck reaction. *Chem. Eur. J.* **6**, 1773–1780 (2000).
5. Yu, D. Y. & Zhang, Y. G. Copper- and copper-*N*-heterocyclic carbene-catalyzed C-H activating carboxylation of terminal alkynes with CO_2 at ambient conditions. *PNAS* **107**, 20184–20189 (2010).
6. Choi, J., Yang, H. Y., Kim, H. J. & Son, S. U. Organometallic hollow spheres bearing bis(*N*-Heterocyclic carbene)–palladium species: catalytic application in three-component Strecker reactions. *Angew. Chem. Int. Ed.* **49**, 7718–7722 (2010).
7. Zhang, C. *et al.* Main-chain organometallic microporous polymers based on triptycene: synthesis and catalytic application in the Suzuki–Miyaura coupling reaction. *Chem. Eur. J.* **19**, 5004–5008 (2013).
8. Kong, G. Q., Ou, S., Zou, C. & Wu, C. D. Assembly and post-modification of a metal-organic nanotube for highly efficient catalysis. *J. Am. Chem. Soc.* **134**, 19851–19857 (2012).
9. Xu, Y. H. *et al.* Conjugated microporous polymers: design, synthesis and application. *Chem. Soc. Rev.* **42**, 8012–8031 (2013).

10. Zou, X. Q., Ren, H. & Zhu, G. S. Topology-directed design of porous organic frameworks and their advanced applications. *Chem. Commun.* **49**, 3925–3936 (2013).
11. Leuthüßer, S., Schwarz, D. & Plenio, H. Tuning the electronic properties of *N*-heterocyclic carbenes. *Chem. Eur. J.* **13**, 7195–7203 (2007).
12. Cho, H. C. *et al*. Tubular microporous organic networks bearing imidazolium salts and their catalytic CO2 conversion to cyclic carbonates. *Chem. Commun.* **47**, 917–919 (2011).
13. Rose, M. *et al*. *N*-Heterocyclic carbene containing element organic frameworks as heterogeneous organocatalysts. *Chem. Commun.* **47**, 4814–4816 (2011).
14. Zhang, Y. G. *et al*. Colloidal poly-imidazolium salts and derivatives. *Nano Today* **4**, 13–20 (2009).
15. Park, K. H., Ku, I., Kim, H. J. & Son, S. U. NHC-based submicroplatforms for anchoring transition metals. *Chem. Mater.* **20**, 1673–1675 (2008).
16. Leuthäußer, S., Schwarz, D. & Plenio, H. Tuning the electronic properties of *N*-heterocyclic carbenes. *Chem. Eur. J.* **13**, 7195–7203 (2007).
17. Agrigento, P. *et al*. Highly cross-linked imidazolium salt entrapped magnetic particles-preparation and applications. *J. Mater. Chem.* **22**, 20728–20735 (2012).
18. Hu, S. & Wang, X. Ultrathin nanostructures: smaller size with new phenomena. *Chem. Soc. Rev.* **42**, 5577–5594 (2013).
19. Jeon, Y. M. *et al*. Amorphous infinite coordination polymer microparticles: a new class of selective hydrogen storage materials. *Adv. Mater.* **20**, 2105–2110 (2008).
20. Li, L. Y., Chen, Z. L., Zhong, H. & Wang, R. H. Urea-based porous organic frameworks: effective supports for catalysis in neat water. *Chem. Eur. J.* **20**, 3050–3060 (2014).
21. Wang, X. S. *et al*. A mesoporous metal-organic framework with permanent porosity. *J. Am. Chem. Soc.* **128**, 16474–16475 (2006).
22. Zhang, Y. G. & Riduan, S. N. Functional porous organic polymers for heterogeneous catalysis. *Chem. Soc. Rev.* **41**, 2083–2094 (2012).
23. García, A. *et al. Org. Lett.* New building block for *C*3 symmetry molecules: synthesis of *s*-triazine-based redox active chromophores. **11**, 5398–5401 (2009).
24. Masciocchi, N. *et al*. Structural and thermodiffractometric analysis of coordination polymers. part I: tin derivatives of the bim ligand [Bim = bis(1-imidazolyl)methane]. *Inorg. Chem.* **46**, 10491–10500 (2007).
25. Park, K. H., Choi, J., Kim, H. J. & Son, S. U. Synthesis of antimony sulfide nanotubes with ultrathin walls via gradual aspect ratio control of nanoribbons. *Chem. Mater.* **19**, 3861–3863 (2007).
26. Chun, J. *et al*. Tubular-shape evolution of microporous organic networks. *Chem. Mater.* **24**, 3458–3463 (2012).
27. Kang, N. *et al*. Nanoparticulate iron oxide tubes from microporous organic nanotubes as stable anode materials for lithium ion batteries. *Angew. Chem. Int. Ed.* **51**, 6626–6630 (2012).

Acknowledgments

This work was financially supported by 973 Program (2011CBA00502), Natural Science Foundation of China (21273239), Natural Science Foundation of Fujian Province (2011J01064) and "One Hundred Talent Project" from Chinese Academy of Sciences.

Author contributions

R. W. and H. Z. designed the research. H. Z., L. L. and Y. W. carried out syntheses and the measurements. All authors discussed the results and commented on the manuscript.

Additional information

Supplementary information accompanies this paper at http://www.nature.com/scientificreports

Competing financial interests: The authors declare no competing financial interests.

How to cite this article: Zhao, H., Li, L., Wang, Y. & Wang, R. Shape-Controllable Formation of Poly-imidazolium Salts for Stable Palladium *N*-Heterocyclic Carbene Polymers. *Sci. Rep.* **4**, 5478; DOI:10.1038/srep05478 (2014).